

Self-driven Hybrid Atom Spin Oscillator

Erwei Li,^{1,2,*} Qianjin Ma,^{1,2,*} Guobin Liu,^{1,2,†} Peter Yun,^{1,2} and Shougang Zhang^{1,2}

¹National Time Service Center, Chinese Academy of Sciences, Xi'an, 710600, China.

²University of Chinese Academy of Sciences, Beijing, 100049, China

(Dated: January 31, 2023)

A self-driven hybrid atom spin oscillator is demonstrated in theory and experiment with a vapor Rb-Xe dual-spin system. The raw signal of Rb spin oscillation is amplified, phase-shifted and sent back to drive the Xe spins coherently. By fine tuning the driving field strength and phase, a self-sustaining spin oscillation signal with zero frequency shift is obtained. The effective coherence time is infinitely prolonged beyond the intrinsic coherence time of Xe spins, forming a hybrid atom spin oscillator. Spectral analysis indicates that a frequency resolution of 13.1 nHz is achieved, enhancing the detection sensitivity for magnetic field. Allan deviation analysis shows that the spin oscillator can operate in continuous wave mode like a spin maser. The prototype spin oscillator can be easily implanted into other hybrid spin systems and enhance the detection sensitivity of alkali metal-noble gas comagnetometers.

Alkali metal-noble gas comagnetometer has been used for both fundamental and practical applications, such as the search for axion like particles or new physics beyond the standard model [1–4] and inertial navigation gyroscope[5–7]. It is important for the comagnetometer to continuously improve the detection sensitivity to magnetic field or angular velocity, to beat the frequency or energy limits at record-breaking measurements [3, 8, 9]. Basically, comagnetometer sensitivity is determined by two main factors, the coherence time and signal to noise ratio (SNR) of the spin oscillation signal.

To improve the SNR, various parametric modulations together with lock-in detection are regularly utilized to suppress the noise [3, 9–11]. Signal can be amplified using smart optical design such as the multi-pass vapor cell [12, 13]. As for the coherence time, increasing the spin longitudinal relaxation time is the first consideration. Buffer gas filling [14] and anti-relaxation paraffin coating [15] in vacuum atomic vapor cell have long been used in the atomic clocks and magnetometers, so the techniques are inherited naturally by alkali metal-noble gas comagnetometers. Multiple spatial or temporal spin-field interaction, such as the well known separated oscillating fields (producing the well known Ramsey fringe in atom fountain clocks) [16], Hahn-echo or spin-echo, CPMG pulse excitation techniques in nuclear magnetic resonance (NMR) spectroscopy [17–19] can also effectively increase the transverse relaxation time or coherence time of spin oscillations.

Inspired by the self-oscillating NMOR magnetometer by Kitching et al. [20], following the feedback oscillator electronics and ac magnetic field excitation NMR, we have been long wondering whether a self-sustaining spin oscillator based on alkali metal-noble gas comagnetometer is possible. Compared to the magnetometer using

pure alkali metal atoms, an alkali metal-noble gas comagnetometer has the advantage of much longer nuclear spin relaxation time, typically from tens of seconds to even hours for example ³He [21], and the nuclear spin coherence can be transferred to alkali atom spin in the hybrid spin dynamics [22]. It is thus theoretically easier for such a system to become self-oscillating given proper feedback conditions.

We consider a model Rb-Xe comagnetometer under the self-feedback or self-driving mode, where the driven spin dynamics can be described by the coupled Bloch equations

$$\begin{aligned}\frac{\partial \mathbf{M}^{\text{Rb}}}{\partial t} &= \frac{\gamma_{\text{Rb}}}{q} \mathbf{M}^{\text{Rb}} \times (\mathbf{B}_0 + \lambda \mathbf{M}^{\text{Xe}}) \\ &\quad + \frac{M_0^{\text{Rb}} \hat{z} - \mathbf{M}^{\text{Rb}}}{q T^{\text{Rb}}}, \\ \frac{\partial \mathbf{M}^{\text{Xe}}}{\partial t} &= \gamma_{\text{Xe}} \mathbf{M}^{\text{Xe}} \times (\mathbf{B}_0 + \lambda \mathbf{M}^{\text{Rb}} + G M_x^{\text{Rb}} e^{i\theta} \hat{y}) \\ &\quad + \frac{M_0^{\text{Xe}} \hat{z} - \mathbf{M}^{\text{Xe}}}{T^{\text{Xe}}}.\end{aligned}\tag{1}$$

where \mathbf{M} is the spin magnetization, M_0 is the initial spin magnetization, \mathbf{B}_0 is the static magnetic field, T is the spin relaxation time. q is the slowing down factor due to Rb-Xe spin exchange collisions in high temperature. λ is the enhancement factor due to Fermi contact interaction between Rb valence electrons and Xe nuclei [22]. Other unspecified notations and the numerical solving procedure can be referred to our previous work in [23].

The driving term $G M_x^{\text{Rb}} e^{i\theta} \hat{y}$ is the phase-shifted spin oscillation of Rb spins in transverse direction and then it couples with Xe spins transversely like a conventional NMR excitation pulse protocol. In this case, the comagnetometer can be regarded as a self-driven hybrid atom spin system and equivalent spin dynamics is: first the fast relaxing Rb spins adiabatically follow the slow precessing Xe spins at certain conditions [24], i.e. the Rb spins act as a probe for Xe spin precession with a little back-action causing minor frequency shift on the Xe spin oscillation; secondly, the Rb spin oscillation signal

* These authors contributed equally to this work and should be regarded as co-first authors.

† liuguobin@ntsc.ac.cn

is amplified, phase shifted and sent back to drive the Xe spins as an ac magnetic field. The driving field strength is determined by the gain factor G and the driving field is in-phase or out of phase depending on the phase shift θ .

The comagnetometer works in two modes: open-loop mode ($G=0$) and close-loop mode ($G\neq 0$). In close-loop mode, the self-driving comagnetometer can work in two different states depending on the magnitude of G . In classical oscillator electronics, a close loop system can be made self-oscillating when product of the gain and feedback approaches one. In simulation, we found a similar critical condition for the close loop comagnetometer to become self-oscillating, which in this case is described as

$$10GM_0^{\text{Rb}} = M_0^{\text{Xe}}, \quad (2)$$

meaning the self-oscillating can be triggered when the driving field strength is about one tenth of the initial Xe spin magnetization. This is easier to be realized compared to the classical self-oscillating oscillator, which can be attributed to the long intrinsic coherence time of Xe spins.

Generally, the self-driving field strength can be divided into two regions: 1) When $10GM_0^{\text{Rb}} \leq M_0^{\text{Xe}}$, the self-driving field is said to be weak since the Xe spin oscillation decays exponentially as usual; 2) When $10GM_0^{\text{Rb}} \geq M_0^{\text{Xe}}$, the self-driving effect becomes strong and a self-sustaining spin oscillation emerges, with an effective coherence time far longer than the intrinsic spin relaxation time of ^{129}Xe spins in typical temperature and buffer gas conditions, as shown by the two insets in Fig.1. As the alkali metal atomic spin magnetization is $\sim 10^3$ times weaker than the noble gas atomic spin magnetization in typical experimental conditions [22], the critical G value is around a few hundreds.

The phase is also critically important in realization of the self-sustaining spin oscillation. Simulation results show that the self-sustaining oscillation can persist for a phase range determined by

$$\theta_0 < \theta < 180^\circ - \theta_0, \quad (3)$$

as indicated by the two sharp structures in the frequency-phase (dispersions) and amplitude-phase (steps) diagrams in Fig.1. The greater the G , the smaller the θ_0 , meaning a wider phase range for self-sustaining oscillation exists given stronger self-driving field.

It is also shown in Fig.1(b), the frequency shifts almost linearly with θ in most of the self-sustaining oscillation phase range given by Eq.3 except at around the critical phase points at θ_0 and $180^\circ - \theta_0$. The shift can be explained as follows, due to the well known Bloch-Siegert shift effect in NMR spectra [25], the mismatch of the initial phase values between the driving field signal and open loop signal can lead to an accumulation effect, which may keep changing gradually the close loop frequency. Therefore one therefore may consider the self-driving comagnetometer not in favor of precision measurement purpose

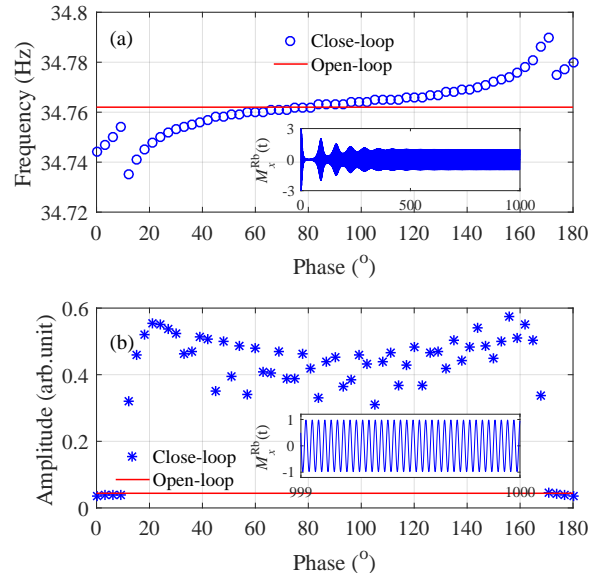


FIG. 1. (color online) Simulated self-driving spin oscillation signal (a) in close loop mode and its frequency response as a function of the self-driving phase shift θ at a fixed strong gain $G=1000$ (b). The cross points between the open-loop curve (red line) and the close-loop curve (blue circles) indicate there are several phase points where zero frequency shift (ZFS) occurs albeit the presence of Bloch-Siegert shift effect under strong off-resonance self-driving field.

albeit the potential gain in signal amplification and coherence time.

However, by numerically solving the Eq.1, we find a phase point where the spin oscillation frequency shift vanishes. As shown in Fig.1(a), the frequency of close-loop (blue circles) crosses with that of open-loop (red line), implying that frequency shift vanishes at certain phase value. Due to Bloch-Siegert shift effect, this zero frequency shift (ZFS) phase θ_{ZFS} is about several degrees below 90° , which is the theoretically in-phase driving phase value consider the y -axis excitation and x -axis detection configuration. The position of θ_{ZFS} depends also on G . The larger the G , the further the θ_{ZFS} away from 90° . The existence of the ZFS phase is important as we have to rule out any possible non-systematic frequency shift sources [8] to find out the fundamentally unknown spin-dependent interactions.

To testify above simulation results, we have constructed a Rb-Xe comagnetometer setup and specially designed the driving electronics with tunable gain and phase parameters, as depicted in Fig.2.

The main part is a typical Rb-Xe comagnetometer, with a vacuum atomic vapor cell containing Rb-Xe mixture gas at high temperature ($\sim 120^\circ\text{C}$) as the atom spins media. A circularly polarized 795 nm laser along the z direction shines into the cell to align the Rb atom spins.

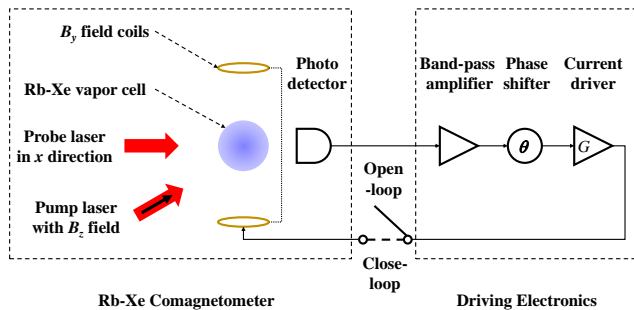


FIG. 2. Experimental schematic of the self-driving Rb-Xe spin oscillator. It consists of a typical pump-probe Rb-Xe comagnetometer (left) and a driving electronics with tunable gain and phase parameters (right). The pump and probe laser powers are 54 mW and 3 mW, respectively. The static field B_z is ~ 30 mG, corresponding to a ^{129}Xe spin oscillation frequency $\nu_0 \sim 35$ Hz.

Then the Rb spin polarization was then transferred to Xe atoms spins via rapid spin-exchange collisions [26]. The polarized Xe spins drive Rb spins in a classical way [24] and at last a linearly polarized 780 nm laser along the x direction reads out the Rb spin dynamics over time as the comagnetometer original output signal.

The driving electronics is basically a combination of a band-pass amplifier, a phase shifter and a current driver. Two factors affects the design of driving electronics. First, the Rb spins have larger response to Xe spins in lower frequency. Secondly, for typical applications including magnetic field and rotation rate measurements, the Rb-Xe comagnetometer works usually in ultra-low frequency range. Both factors urge the target spin oscillation to be at the range from several hertz to a few tens of hertz. Unfortunately, the $1/f$ law of noise spectra indicate the spin oscillation signal may be easily disturbed by loud amplitude and phase noises at the frequency range. While the gain G has high tuning resolution, the phase resolution $\Delta\theta$ is limited to a few degrees although the driving electronics is custom made with special design in noise reduction.

For one typical experimental cycle, we first break the link between the Rb-Xe comagnetometer and driving electronics and record an open-loop spin oscillation signal, as shown in Fig.3(a). Then we restore the link, set the electronics driving output at a fix gain and change the phase point by point with an accuracy of a few degrees, recording the spin oscillation signals accordingly. At last, we fix the phase to the ZFS point where the close-loop spin oscillation frequency coincides with the open-loop one and record a long-time spin oscillation signal, as shown in Fig.3(b).

With standard Fourier analysis and data fitting process, we extract the spin oscillation frequency versus phase and find it agree with the simulation results in

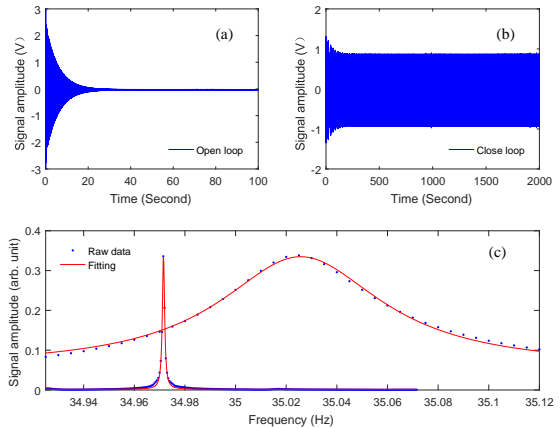


FIG. 3. (color online) Spin oscillation signals of the self-driving Rb-Xe spin oscillator in open-loop (a) and close-loop (b) modes, and the corresponding Fourier spectra comparison (c). A linewidth narrowing by a factor of 75 and SNR enhancement by a factor of 34 is achieved when switching from the open loop to close loop modes. The open loop Fourier spectra in (c) was amplified by ten times for increasing the visibility.

Fig.1(b). As shown in Fig.3(c), a spectral linewidth of 0.04 Hz with $\text{SNR} \sim 1200$ and a spectral linewidth of 0.53 mHz with $\text{SNR} \sim 40600$ are obtained for the open loop and close loop signals, respectively. Compared to the open loop operation, the frequency resolution of the ^{129}Xe spin resonance frequency was improved by a factor of ~ 2540 , from $33.3 \mu\text{Hz}$ down to 13.1 nHz , approaching the state of the art accuracy [3]. For ^{129}Xe with gyromagnetic ratio 11.78 MHz/T , this level of frequency resolution leads to a magnetic field resolution of $\approx 1.11 \text{ fT}$, sufficient for applications such as the detection of human brain magnetic field [27].

It shall be noted that the center frequency of close-loop and open-loop signals does not coincide exactly with each other due to the limited tuning resolution of phase control by rheostats in present experiment. This shall be easily improved with higher phase tuning techniques, such as a direct digital synthesis (DDS).

We have been observing the spin oscillation signal with a real-time oscilloscope for hours and found no sign of decaying at all, indicating the effective coherence time of spin oscillation probably being infinite. Once the loop is open, the spin oscillation starts to decay exponentially again within the intrinsic coherence time of noble gas spin. In this sense, the self-driving comagnetometer can be taken as a hybrid atomic spin oscillator, preferably working in continuous wave mode like conventional laser or maser.

To test the performance of hybrid spin oscillator in long term operation, we recorded continuously the spin oscillation for 10000 seconds in the close loop operation and

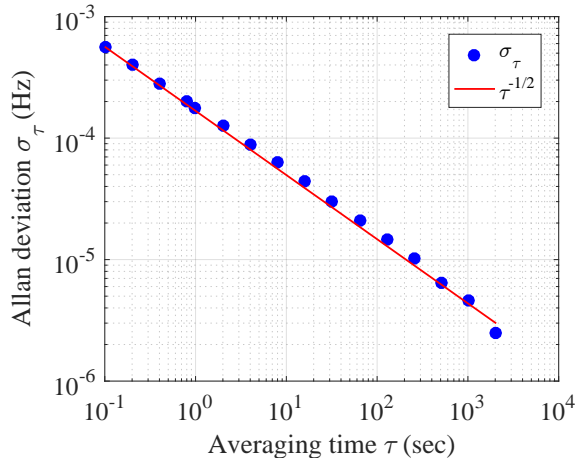


FIG. 4. (color online) Allan deviation of the ^{129}Xe spin oscillation frequency in averaging time up to 1000 seconds. A frequency instability of $2.99 \mu\text{Hz}$ is achieved at a measuring time of 2048 seconds, equivalent to a bias instability of $3.87^\circ/\text{h}$.

excuted a standard Allan deviation analysis for the last 9000 seconds, as shown in Fig.4. The frequency instability of spin oscillation reaches $2.99 \mu\text{Hz}$ at 2048 seconds averaging time, equivalent to a bias instability of $\sim 3.87^\circ/\text{h}$ for gyroscopic measurement.

With respect to the 13.1 nHz frequency resolution, the $2.99 \mu\text{Hz}$ frequency instability is relatively high. We attributed this deterioration to various frequency drift sources. For example, we observed for two days a correlation between the drift of spin oscillation frequency (at 10^{-4} level) and the drift of heater power for vapor cell, which was a result of the slowly varying residual magnetic field produced by the leaky current of the heater wires. Besides, the pump laser power is in free running mode, whose fluctuation can cause significant fluctuation (at 1% level) of the optical pumping rate thus the fluctuation of alkali atom spin magnetization, which finally cause the frequency shift of the noble gas spin oscillation. There are other factors affecting the middle to long term frequency instability, such as the drift of current feeding the bias field coils.

As indicated by Fig.1(a), the fluctuation of unlocked phase can also lead to a frequency shift with a slope of $\delta\nu/\delta\theta \sim 10^{-4} \text{ Hz}/^\circ$. A possible improvement is to use phase-lock method [28] to lock the driving phase at the ZFS point. Considering the infinite effective coherence

time, the self-driving spin oscillator has the potential to reach a frequency instability at nHz level at long term running. As shown by Fig.4, the σ_τ continues going down at 2048 seconds, indicating a better frequency instability can be reached given longer running time.

During the process of preparing the manuscript, we noticed the work by Jiang et al.[29], which presented similar phenomena. We have to emphasize the following important differences between their work and ours. First, we built the spin oscillator with a simpler prototype setup, neither external driving field nor parametric modulation (together with lock-in detection) is used in experiment and no significant SNR loss observed. Secondly, we derived the self-oscillating conditions for Rb-Xe comagnetometer by developing a different theoretical framework, especially the introduction of G and θ parameters, which are conceptually convenient for understanding and easier to be used for guiding experiment. At last, we found the existence of zero frequency shift phase in theory and experiment, which is important for various applications in precision measurement physics.

In principle, the demonstrated self-driving spin oscillator scheme can be also applied to other dual-spin system, such as the K- ^3He comagnetometer, and also to the trispin comagnetometer, such as the Rb- ^3He - ^{129}Xe or Rb- ^{129}Xe - ^{131}Xe configuration [3, 13] with careful design of dual-channel driving electronics with respect to the two noble gas spin oscillation frequencies.

In conclusion, we have demonstrated theoretically and experimentally a self-driving spin oscillator based on the Rb-Xe comagnetometer. A self-sustaining oscillator with prolonged coherence time can be realized at strong self-driving condition. The spin oscillation frequency shift can vanish at certain phase points albeit the Bloch-Siegert shift effect. The frequency resolution of the hybrid spin oscillator reaches several nHz level, potentially enhancing the detection sensitivity for magnetic or gyroscopic measurements with a simple apparatus. With further improvement on the frequency instability, the hybrid atomic spin oscillator can work like laser or maser for long term operation, promising for various scientific or practical applications, such as the searching for new spin-dependent interactions and earth rotation monitoring.

The author Guobin Liu would like to thank Dong Sheng and Min Jiang from the University of Science and Technology of China for helpful discussions. The authors also appreciate the financial support by the Chinese Academy of Sciences under grant no E209YC1101 and by the National Time Service Center under grant no E024DK1S01.

[1] M. Bulatowicz, R. Griffith, M. Larsen, J. Mirijanian, C. B. Fu, E. Smith, W. M. Snow, H. Yan, and T. G. Walker, *Phys. Rev. Lett.* **111**, 102001 (2013).

[2] M. Pospelov, S. Pustelny, M. P. Ledbetter, D. F. Jackson Kimball, W. Gawlik, and D. Budker, *Phys. Rev. Lett.* **110**, 021803 (2013).

- [3] M. E. Limes, D. Sheng, and M. V. Romalis, *Phys. Rev. Lett.* **120**, 033401 (2018).
- [4] N. Sachdeva, I. Fan, E. Babcock, M. Burghoff, T. E. Chupp, S. Degenkolb, P. Fierlinger, S. Haude, E. Kraegeloh, W. Kilian, S. Knappe-Grüneberg, F. Kuchler, T. Liu, M. Marino, J. Meinel, K. Rolfs, Z. Salhi, A. Schnabel, J. T. Singh, S. Stuißer, W. A. Terrano, L. Trahms, and J. Voigt, *Phys. Rev. Lett.* **123**, 143003 (2019).
- [5] E. A. Donley, *2010 IEEE Sensors*, 17 (2010).
- [6] T. W. Kornack, R. K. Ghosh, and M. V. Romalis, *Phys. Rev. Lett.* **95**, 230801 (2005).
- [7] T. G. Walker and M. S. Larsen, *Advances in Atomic Molecular and Optical Physics* **65**, 373 (2016).
- [8] W. A. Terrano, J. Meinel, N. Sachdeva, T. E. Chupp, S. Degenkolb, P. Fierlinger, F. Kuchler, and J. T. Singh, *Phys. Rev. A* **100**, 012502 (2019).
- [9] A. Almasi, J. Lee, H. Winarto, M. Smiciklas, and M. V. Romalis, *Phys. Rev. Lett.* **125**, 201802 (2020).
- [10] D. Budker, W. Gawlik, D. F. Kimball, S. M. Rochester, V. V. Yashchuk, and A. Weis, *Rev. Mod. Phys.* **74**, 1153 (2002).
- [11] D. A. Thrasher, S. S. Sorensen, J. Weber, M. Bulatowicz, A. Korver, M. Larsen, and T. G. Walker, *Phys. Rev. A* **100**, 061403(R) (2019).
- [12] S. Li, P. Vachaspati, D. Sheng, N. Dural, and M. V. Romalis, *Phys. Rev. A* **84**, 061403(R) (2011).
- [13] C.-P. Hao, Q.-Q. Yu, C.-Q. Yuan, S.-Q. Liu, and D. Sheng, *Phys. Rev. A* **103**, 053523 (2021).
- [14] H. G. Dehmelt, *Phys. Rev.* **105**, 1487 (1957).
- [15] M. A. Bouchiat and J. Brossel, *Physical Review* **147**, 41 (1966).
- [16] N. F. Ramsey, *Phys. Rev.* **76**, 996 (1949).
- [17] E. L. Hahn, *Phys. Rev.* **80**, 580 (1950).
- [18] S. Meiboom and D. Gill, *Review of Scientific Instruments* **29**, 688 (1958).
- [19] M. H. Levitt, *Spin dynamics: basics of nuclear magnetic resonance* (Wiley, 2001).
- [20] P. D. D. Schwindt, L. Hollberg, and J. Kitching, *Review of Scientific Instruments* **76**, 126103 (2005).
- [21] T. R. Gentile, P. J. Nacher, B. Saam, and T. G. Walker, *Rev. Mod. Phys.* **89**, 045004 (2017).
- [22] T. W. Kornack and M. V. Romalis, *Phys. Rev. Lett.* **89**, 253002 (2002).
- [23] G. Liu, *Phys. Rev. A* **99**, 033409 (2019).
- [24] G. Liu, V. Guarrera, S. Gu, and S. Zhang, *Phys. Rev. A* **104**, 032827 (2021).
- [25] F. Bloch and A. Siegert, *Phys. Rev.* **57**, 522 (1940).
- [26] T. G. Walker and W. Happer, *Rev. Mod. Phys.* **69**, 629 (1997).
- [27] H. Xia, A. Ben-Amar Baranga, D. Hoffman, and M. V. Romalis, *Applied Physics Letters* **89**, 211104 (2006).
- [28] K. Zhang, N. Zhao, and Y. H. Wang, *Scientific Reports* **10**, 2258 (2020).
- [29] M. Jiang, H. Su, Z. Wu, X. Peng, and D. Budker, *Science Advances* **7**, eabe0719 (2021).